

## Correlations between Optical Variability and Physical Parameters of Quasars

Wenwen Zuo<sup>1</sup>, Xue-Bing Wu<sup>1,\*</sup>, Yi-Qing Liu<sup>1</sup> & Cheng-Liang Jiao<sup>2</sup>

<sup>1</sup>*Department of Astronomy, Peking University, Beijing 100871, China.*

<sup>2</sup>*Korea Astronomy and Space Science Institute, Daejeon, South Korea.*

\**e-mail: wuxb@pku.edu.cn*

**Abstract.** Optical variability is an important feature of quasars. Taking advantage of a larger sample of 7658 quasars from SDSS Stripe 82 and relatively more photometric data points for each quasar, we estimate their variability amplitudes and divide the sample into small bins of various parameters. An anticorrelation between variability amplitude and rest-frame wavelength is found. Variability increases as either luminosity or Eddington ratio decreases. The relationship between variability and black hole mass is uncertain. The intrinsic distribution of variability amplitudes for radio-loud and radio-quiet quasars are different. Both radio-loud and radio-quiet quasars exhibit a bluer-when-brighter chromatism. With the Shakura–Sunyaev disk model, we find that changes of accretion rate play an important role in producing the observed optical variability. However, the predicted positive correlation between variability and black hole mass seems to be inconsistent with the observed negative correlation between them in small bins of Eddington ratio, which suggests that other physical mechanisms may still need to be considered in modifying the simple accretion disk model. The different mechanisms in radio-loud and radio-quiet quasars are discussed.

*Key words.* Accretion, accretion disks—galaxies: active—galaxies: nuclei—quasars: general.

### 1. Introduction

Variability is one of the major characteristics of Active Galactic Nuclei (AGNs), whose luminosities vary in all the bands from  $\gamma$ -ray to radio, on timescales from hours to years. Although the study of variability plays an important role in investigating the nature of the compact central region in AGNs (Vanden Berk *et al.* 2004; Wilhite *et al.* 2008), the mechanism underlying quasar variability is still inconclusive. To clarify the nature of quasar variability, most previous studies focussed on the dependencies of the variability indicator on redshift, time lag, rest-frame wavelength and luminosity (Vanden Berk *et al.* 2004; Wilhite *et al.* 2008; MacLeod *et al.* 2010). We revisit the correlations between the variability amplitude and physical

parameters based on a sample of 7658 quasars in SDSS Stripe 82 (MacLeod *et al.* 2010; Sesar *et al.* 2007), with both the individual variability method and detailed parameter binning techniques. Black hole masses, bolometric luminosities and Eddington ratios of them are obtained from the quasar catalogue in Shen *et al.* (2011). More details about these correlations can be found in Zuo *et al.* (2012).

## 2. Quasar sample and variability estimation

A sample of 9254 variable quasars is obtained from cross-matching the spectroscopic confirmed SDSS DR7 quasars (Schneider *et al.* 2010; Shen *et al.* 2011) and a sample of 67507 variable sources in SDSS Stripe 82 (MacLeod *et al.* 2010; Ivezić *et al.* 2007; Sesar *et al.* 2007), which lies along the celestial equator in the southern galactic hemisphere ( $\sim 22\text{ h } 24\text{ m} < \alpha_{J2000} \lesssim 04\text{ h } 08\text{ m}$ ,  $-1.27^\circ < \delta_{J2000} < +1.27^\circ$ ,  $\sim 290\text{ deg}^2$ ) and have repeated photometric observations (at least 4 per band, with a median of 10) measured up to 10 years in the  $u'g'r'i'z'$  system (Fukugita *et al.* 1996). Black hole mass, bolometric luminosity and Eddington ratio are obtained from the quasar catalogue of Shen *et al.* (2011), where black hole mass of quasars are settled on fiducial virial mass estimates:  $H_\beta$  estimates for  $z < 0.7$  (Vestergaard & Wilkes 2006), MgII estimates for  $0.7 \leq z < 1.9$  (Shen & Kelly 2010) and CIV estimates for  $z \geq 1.9$  (Vestergaard & Wilkes 2006). If more than one emission lines are available, we still adopt the fiducial virial black hole mass in Shen & Kelly (2010). 99% of quasars have measurable quantity. To measure the variability amplitude in each filter band for every quasar, we adopt the formalism similar to that used in Ai *et al.* (2010) and Sesar *et al.* (2007).

## 3. Variability distribution and colour change

Since the physical origin of optical variability in radio-quiet and radio-loud quasars are different (Giveon *et al.* 1999), among the 9254 quasars, we divide 7890 quasars with either radio detections or in the fields of FIRST radio survey into two subsamples (White *et al.* 1997). Radio-quiet subsample contains quasars with radio loudness  $< 10$ ; radio-loud subsample holds quasars with radio loudness  $> 10$ .

438 radio-loud sources and 7452 radio-quiet sources are obtained, but only 424 radio-loud and 7314 radio-quiet quasars have reliable variability indicators in the  $g'$ ,  $r'$  and  $i'$  bands, which means that variability in each band for a quasar is a non-zero value estimated from at least 10 data points, even after eliminating photometric outliers. In addition, 8 radio-loud and 72 radio-quiet quasars are rejected due to the unmeasurable black hole mass (Shen & Kelly 2010). Thus, 416 radio-loud and 7242 radio-quiet quasars are studied in the following sections.

The variability amplitudes of radio-quiet and radio-loud quasars are mostly distributed between 0.05 and 0.3, except that there is a relatively higher fraction of radio-loud quasars ( $\sim 2.96\%$ ) with variability amplitudes  $> 0.3$  compared to radio-quiet quasars ( $\sim 1.73\%$ ). The median variability amplitude of radio-quiet objects is almost similar compared to radio-loud quasars. However, their distributions differ significantly from the Kolmogorov–Smirnov (KS) tests ( $p \sim 0.012$ ). We randomly divide both the radio-quiet and radio-loud quasar samples 100 times and found

different distributions. Here we take the magnitude difference between two adjacent SDSS filter bands as the colour indicator. Using the data in  $g'$ ,  $r'$  and  $i'$  filter bands, we can get 2 colours, viz.  $g'-r'$  and  $r'-i'$ . Both radio-quiet and radio-loud quasars display a strong bluer-when-brighter chromatism.

#### 4. Correlations between variability and quasar parameters

As the quasar variability amplitude depends on quasar luminosity ( $L_{\text{bol}}$ ), rest-frame wavelength ( $\lambda_{\text{rf}}$ ), black hole mass ( $M_{\text{BH}}$ ) and possibly redshift ( $z$ ), such dependences can be formulated as  $V(\lambda_{\text{rf}}, z, M_{\text{BH}}, L_{\text{bol}})$ , where the combination of dependences of the variability amplitude on  $M_{\text{BH}}$  and  $L_{\text{bol}}$  can be replaced by the combination of its dependences on  $M_{\text{BH}}$  and  $R_{\text{EDD}}$  (Eddington ratio) or that on  $R_{\text{EDD}}$  and  $L_{\text{bol}}$ . The dependence of variability amplitude on each parameter can be obtained in subsamples where other parameters are constrained within small ranges. Supposing that  $X$  is one of the five parameters ( $\lambda_{\text{rf}}, z, M_{\text{BH}}, L_{\text{bol}}, R_{\text{EDD}}$ ), the Spearman's correlation coefficient  $r1\_X$  is calculated in each corresponding subsample or sub-subsample to describe the rank correlation, while the significance  $p\_X$  of its value deviating away from 0 is also obtained. To parametrize the observed relation between the variability amplitude and the parameter  $X$ , we fit all the data in each subsample with a simple function:

$$V(X) = b\_X \log X + a\_X. \quad (1)$$

Accompanied by the slope  $b\_X$  and y-axis intercept value  $a\_X$ , the Pearson product-moment correlation coefficient  $r2\_X$  is also calculated to illustrate the strength of the proposed relation ( $r2\_X$  for short). In the following sections,  $X$  will be replaced with  $\lambda_{\text{rf}}, z, M_{\text{BH}}, L_{\text{bol}}$ , and  $R_{\text{EDD}}$ .

The median values for the relationships between  $V$  and different quasar parameters are summarized in Table 1. There is an anticorrelation between the variability amplitude and rest-frame wavelength after excluding influence of redshift and the intrinsic parameters on variability amplitude. There is almost no correlation between the variability amplitude and redshift after excluding influence of other parameters. The variability amplitude is significantly anticorrelated with  $R_{\text{EDD}}$  and  $L_{\text{bol}}$  in subsamples without binning in quasar parameters. There is no certain correlation between variability and  $M_{\text{BH}}$  in all these subsamples. After considering relationships among intrinsic quasar parameters, we find that small data sets still exhibit an anticorrelation between variability and  $R_{\text{EDD}}$ , and between variability and  $L_{\text{bol}}$  with a lower significance level. Moreover, an anticorrelation of the variability amplitude with  $M_{\text{BH}}$  begins to emerge in  $R_{\text{EDD}}$  bins and the correlation with  $M_{\text{BH}}$  is shown in  $L_{\text{bol}}$  bins.

#### 5. Implications of standard accretion disk model

Based on the Shakura–Sunyaev model (Shakura & Sunyaev 1973) and assuming the change of accretion rate as the origin of quasar variability (Li & Cao 2008), we calculate the emitted spectra from the accretion disk for different black hole masses and accretion rates. After convolving with SDSS filter response function, we convert the flux to SDSS AB magnitude  $A(M_{\text{BH}}, \dot{m})$ . Assuming the change of  $\dot{m}$  is  $x\dot{m}$ , we

**Table 1.** Correlation between variability and each parameter.

Radio loudness <sup>1</sup>	Parameter <sup>2</sup>	Restricted parameters <sup>3</sup>			Pearson $r^{26}$	Linear fit		
		$x1, x2, x3$	Spearman $r^{14}$	$p^5$		$b^7$	$a^8$	
Radio-quiet	$\log \lambda_{\text{rf}}$	$R_{\text{EDD}}, z, M_{\text{BH}}$	-0.229	0.019	-0.233	-0.137 ± 0.052	0.579 ± 0.180	
Radio-quiet	$\log z$	$R_{\text{EDD}}, M_{\text{BH}}, \lambda_{\text{rf}}$	-0.081	0.189	-0.090	-0.049 ± 0.044	0.131 ± 0.009	
Radio-quiet	$\log L_{\text{bol}}$	$z, R_{\text{EDD}}, \lambda_{\text{rf}}$	-0.269	0.015	-0.260	-0.044 ± 0.020	2.128 ± 0.913	
Radio-quiet	$\log L_{\text{bol}}$	$z, M_{\text{BH}}, \lambda_{\text{rf}}$	-0.343	0.003	-0.335	-0.063 ± 0.020	3.032 ± 0.926	
Radio-quiet	$\log R_{\text{EDD}}$	$z, L_{\text{bol}}, \lambda_{\text{rf}}$	-0.167	0.137	-0.147	-0.020 ± 0.014	0.091 ± 0.011	
Radio-quiet	$\log R_{\text{EDD}}$	$z, M_{\text{BH}}, \lambda_{\text{rf}}$	-0.303	0.013	-0.299	-0.052 ± 0.019	0.075 ± 0.013	
Radio-quiet	$\log M_{\text{BH}}$	$z, L_{\text{bol}}, \lambda_{\text{rf}}$	0.113	0.235	0.104	0.013 ± 0.014	-0.002 ± 0.119	
Radio-quiet	$\log M_{\text{BH}}$	$z, R_{\text{EDD}}, \lambda_{\text{rf}}$	-0.203	0.057	-0.201	-0.033 ± 0.019	0.394 ± 0.168	
Radio-loud	$\log \lambda_{\text{rf}}$	$R_{\text{EDD}}, z, M_{\text{BH}}$	-0.187	0.218	-0.224	-0.225 ± 0.143	0.950 ± 0.494	
Radio-loud	$\log z$	$R_{\text{EDD}}, M_{\text{BH}}, \lambda_{\text{rf}}$	-0.153	0.306	-0.062	-0.034 ± 0.116	0.148 ± 0.028	
Radio-loud	$\log L_{\text{bol}}$	$z, R_{\text{EDD}}, \lambda_{\text{rf}}$	-0.266	0.297	-0.269	-0.058 ± 0.054	2.794 ± 2.456	
Radio-loud	$\log L_{\text{bol}}$	$z, M_{\text{BH}}, \lambda_{\text{rf}}$	-0.384	0.164	-0.321	-0.071 ± 0.055	3.373 ± 2.536	
Radio-loud	$\log R_{\text{EDD}}$	$z, L_{\text{bol}}, \lambda_{\text{rf}}$	-0.304	0.300	-0.274	-0.045 ± 0.032	0.079 ± 0.035	
Radio-loud	$\log R_{\text{EDD}}$	$z, M_{\text{BH}}, \lambda_{\text{rf}}$	-0.369	0.188	-0.291	-0.069 ± 0.047	0.056 ± 0.055	
Radio-loud	$\log M_{\text{BH}}$	$z, L_{\text{bol}}, \lambda_{\text{rf}}$	0.246	0.386	0.212	0.040 ± 0.035	-0.206 ± 0.309	
Radio-loud	$\log M_{\text{BH}}$	$z, R_{\text{EDD}}, \lambda_{\text{rf}}$	-0.220	0.432	-0.180	-0.052 ± 0.052	0.600 ± 0.477	

Notes: <sup>1</sup>The radio-quiet (radio-loud) subsample contains quasars with radio loudness smaller (<) than 10. <sup>2</sup>The parameter on which the dependence of variability is to be considered. <sup>3</sup>Parameters which are restricted in small ranges to exclude their influences on variability, denoted by  $x1, x2$  and  $x3$ .  $4, 5, r1$  is the median value of the Spearman rank correlation coefficients in all the qualified small data sets, while  $p$  is the median value of the significance of its deviation from 0.  $6, r2$  is the median value of the Pearson product correlation coefficient, indicating the strength of linear correlations.  $7, 8, b$  is the median slope of the linear fitting for the dependence of the variability amplitude on the parameter denoted in the column and  $a$  is the median  $y$ -axis intercept of the linear fit.

adopt  $V = A(M_{\text{BH}}, \dot{m}) - A(M_{\text{BH}}, (1+x)\dot{m})$  as variability indicators. We reproduce relationships of the variability amplitude with rest-frame wavelength with good agreement, and tendencies of correlations between variability and  $R_{\text{EDD}}$  as well as  $L_{\text{bol}}$ . The predicted correlation between variability and  $M_{\text{BH}}$  does not seem to correspond well to the case inferred from observations, an anti-correlation with  $M_{\text{BH}}$  in small  $R_{\text{EDD}}$  bins. It implies that the change of accretion rate is important for producing the observed optical variability of quasars but other physical mechanisms

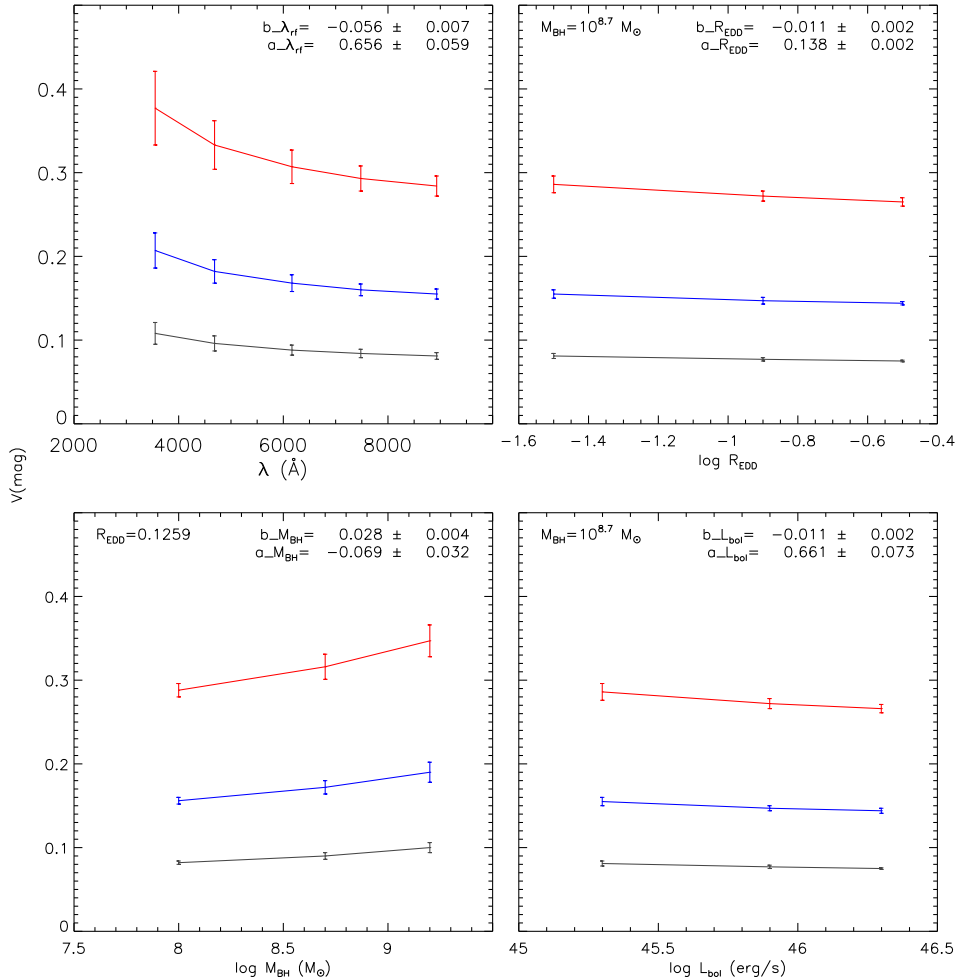


**Figure 1.** The upper left panel shows the model predicted variability amplitude as a function of wavelength, here  $M_{\text{BH}} = 10^{8.7} M_{\odot}$  and  $R_{\text{EDD}} = 0.1259$ ; the upper right panel shows variability amplitude in the  $r'$  band as a function of  $R_{\text{EDD}}$ . The lower left panel shows variability amplitude in the  $r'$  band as a function of  $M_{\text{BH}}$ ; the lower right panel shows variability amplitude in the  $r'$  band as a function of  $L_{\text{bol}}$ . The red, black and blue lines refer to cases with different changes of accretion rate, viz. 0.4, 0.2 and 0.1  $\dot{m}$ . The obtained slope  $b$  for the simulated data during the case with the change of accretion rate at 0.2  $\dot{m}$  are shown in the upper right corner of each panel.

still need to be considered in modifying the simple accretion disk model for quasars (Fig. 1).

In addition, we should keep in mind that radio-loud quasars may have different or additional mechanisms for optical variability, in comparison with radio-quiet quasars. Relativistic jets probably have significant contributions to the optical variability of radio-loud quasars, just as in the case of other blazars.

### Acknowledgement

This work is supported by the National Natural Science Foundation of China (Grant No. 11033001).

### References

- Ai, Y. L., Yuan, W., Zhou, H. Y. *et al.* 2010, *Astrophys. J. Suppl.*, **716**, L31.  
Fukugita, M., Ichikawa, T., Gunn, J. E. *et al.* 1996, *Astron. J.*, **111**, 1748.  
Giveon, U., Maoz, D., Kaspi, S., Netzer, H., Smith, P. S. 1999, *Mon. Not. R. Astron. Soc.*, **306**, 637.  
Ivezić, Ž., Smith, J. A., Miknaitis, G. *et al.* 2007, *Astron. J.*, **134**, 973.  
Li, S.-L., Cao, X. 2008, *Mon. Not. R. Astron. Soc.*, **387**, L41.  
MacLeod, C. L., Ivezić, Ž., Kochanek, C. S. *et al.* 2010, *Astrophys. J.*, **721**, 1014.  
Schneider, D. P., Richards, G. T., Hall, P. B. *et al.* 2010, *Astrophys. J.*, **139**, 2360.  
Sesar, B., Ivezić, Ž., Lupton, R. H. *et al.* 2007, *Astrophys. J.*, **134**, 2236.  
Shakura, N. I., Sunyaev, R. A. 1973, *Astron. Astrophys.*, **24**, 337.  
Shen, Y., Kelly, B. C. 2010, *Astrophys. J.*, **713**, 41.  
Shen, Y., Richards, G. T., Strauss, M. A. *et al.* 2011, *Astrophys. J. Suppl.*, **194**, 45.  
Vanden Berk, D. E., Wilhite, B. C., Kron, R. G. *et al.* 2004, *Astrophys. J. Suppl.*, **601**, 692.  
Vestergaard, M., Wilkes, B. J. 2006, *Astrophys. J.*, **641**, 689.  
White, R. L., Becker, R. H., Helfand, D. J., Gregg, M. D. 1997, *VizieR Online Data Catalogue*, **8048**.  
Wilhite, B. C., Brunner, R. J., Grier, C. J., Schneider, D. P., Vanden Berk, D. E. 2008, *Mon. Not. R. Astron. Soc.*, **383**, 1232.  
Zuo, W., Wu, X.-B., Liu, Y.-Q., Jiao, C.-L. 2012, *Astrophys. J.*, **758**, 104.